T. &A. M. Report No. 404

# PULSE PROPAGATION IN FLUID-FILLED TUBES

by

J. S. Walker and J. W. Phillips

Department of Theoretical and Applied Mechanics
University of Illinois at Urbana-Champaign
Urbana, Illinois 61801

November, 1975

# PULSE PROPAGATION IN FLUID-FILLED TUBES

by

J. S. Walker and J. W. Phillips
Department of Theoretical and Applied Mechanics
University of Illinois

## Abstract

A new theory for the propagation of pressure pulses in an inviscid compressible fluid contained in a thin-walled elastic tube is presented. This theory represents an improvement over the classical waterhammer theory because the restriction that the speed of sound in the tube material must be much greater than that in the fluid has been removed and because the restriction that the pulse length must be much greater than the tube diameter has been somewhat relaxed. The degree to which the latter has been relaxed will be determined by the results of an experimental program currently in progress.

The new theory is applied to a capped tube with an axial impulsive force applied to the capped end for a short period. Numerical solutions using the method of characteristics are presented for a water-filled copper tube and for two different pulse lengths.

An analytical solution is obtained for the special case when the speeds of sound in the tube material and in the fluid are equal and this provides a check on the numerical solution.

## 1. Introduction

To date, acoustic waves in inviscid, compressible liquids contained in elastic tubes have been treated in two ways. The first approach is the classical waterhammer approach (see e.g., Streeter and Wylie [1]), in which the fluid velocity is axial and both it and the pressure are uniform across the tube at each cross section. The inertia of the tube is neglected so that the tube instantaneously expands or contracts until its hoop stress balances the internal pressure. Although radial fluid flow is ignored, the continuity or conservation of mass equation is modified to account for changes in the tube's cross sectional area due to its passive expansion. In this approach the equations are those for plane acoustic waves in an unbounded liquid (see e.g., Walker [2]) with a modified wave speed, i.e., the tube expansion increases the total fluid mass between two adjacent cross sections for a given pressure and thus increases the effective compressibility of the liquid with a corresponding reduction in the apparent wave speed. The modified wave speed is not a true wave speed, i.e., the speed at which a discontinuity travels; at most it represents an engineering approximation to a wave whose leading edge is moving at the true wave speed but whose peak pressure travels at an effectively slower speed because of the wave dispersion associated with the pressure relief provided by the tube expansion. In effect this approach includes the radial fluid velocity term in the continuity equation but ignores corresponding terms in the radial momentum equation.

The second approach (see e.g., Lin and Morgan [3]) represents an attempt to avoid the basic inconsistency in the first approach. The fluid motion is assumed to be axisymmetric, i.e., the velocity has an axial component $v_s$ and a radial component $v_R$, while both these together with the pressure $p$ are functions of the axial coordinate $s$, the radial coordinate $R$ and time $t$. (See Fig. 1). The tube can be treated as a thin shell with inertia so that its motion is described by its radial displacement $w$ and its axial displacement $u$, both of which are functions of $s$ and $t$ only. The fluid and tube problems are coupled by the boundary condition at the inside surface of the tube, namely at $R = r$. For a given problem the Fourier transform variable appears in the arguments of Bessel functions in the transformed solution and the Fourier inversion cannot be obtained without some approximation. Lin and Morgan treat periodic acoustic waves for which the Fourier transform variable is replaced by the unknown wave number and the Fourier inversion is replaced by the problem of solving a dispersion equation involving the same Bessel functions. For wave lengths which are much longer than the tube radius, the Bessel functions can be replaced by their asymptotic expansions for small argument. Using the leading term in each expansion, Lin and Morgan solve for the first two wave numbers. Lin and Morgan also present numerical solutions of their dispersion equation for arbitrary wave length. One sidelight of the results presented by Lin and Morgan is the demonstration that the modified wave speed used in the first approach actually corresponds to the phase speed of long periodic waves when the speed of sound in the tube material is much greater than that in the liquid. Indeed, after the introduction of the long wave length approximation the second approach is similar to the first; the radial velocity is much smaller than the axial one, while the axial velocity and the pressure are nearly uniform across the tube. The principal difference is that the second approach includes the small effects of radial velocity and radial pressure gradient in an asymptotically consistent way and thus avoids the basic inconsistency in the first approach. The greatest disadvantage of the asymptotic approach as it is presented by Lin and Morgan and others is that it appears to require a partial solution of the two-dimensional, unsteady acoustic equation before the asymptotic expansions for long wave length can be introduced.

The object of the present analysis is to begin with an approximation which is equivalent to the long wave length one and to derive equations which govern both the tube and fluid motion and which involve only $s$ and $t$ as independent variables and not $R$. These equations will be as simple as those in the first approach, but will also be as consistent as those in the second approach.

## 2. Equations along characteristics

The equations governing the flow of a compressible inviscid liquid are

$$\partial\rho/\partial t + (\underline{v} \cdot \underline{\nabla})\rho + \rho(\underline{\nabla} \cdot \underline{v}) = 0 , \qquad (1a)$$

$$\rho\, \partial\underline{v}/\partial t + \rho(\underline{v} \cdot \underline{\nabla})\underline{v} + \underline{\nabla} p = 0 , \qquad (1b)$$

$$dp/d\rho = K/\rho , \qquad (1c)$$

where $\rho$, $\underline{v}$ and $p$ are the density, velocity and pressure respectively. The liquid's bulk modulus $K$ is taken to be a constant, which rules out flows in which cavitation occurs. The acoustic assumption is that the velocity is much less than the speed of sound in the liquid,

$$c_f = (K/\rho_f)^{\frac{1}{2}} ,$$

where $\rho_f$ is the liquid's density when there is no motion. With this assumption the second terms in each of the equations (1a, b) can be neglected and the variable $\rho$ can be replaced by the constant $\rho_f$ in the last term of equation (1a), in the first term of equation (1b) and on the right hand side of equation (1c). For axisymmetric flow these equations become

$$(1/K)\,\partial p/\partial t + \partial v_R/\partial R + v_R/R + \partial v_s/\partial s = 0 , \tag{2a}$$

$$\rho_f\,\partial v_R/\partial t + \partial p/\partial R = 0 , \qquad \rho_f\,\partial v_s/\partial t + \partial p/\partial s = 0 , \tag{2b, c}$$

where $v_R$ and $v_s$ are the radial and axial velocity components respectively while $R$ and $s$ are the radial and axial coordinates respectively. (See Fig. 1). Equation (1c) has been used to eliminate $\rho$ from equation (1a).

Lin and Morgan [3] present solutions of equations (2) for periodic disturbances applied at one end of a semi-infinite tube. Each of the variables in their solution is equal to a periodic function of $(s - c_f\, t)$ times $J_o\,(kR)$ or $J_1\,(kR)$ where $J_o$ and $J_1$ are Bessel functions of the first kind and $k$ is the wave number for the disturbance. For disturbances with long wave lengths, $k << r$, where $r$ is the inside radius of the undeformed tube, and the Bessel functions can be replaced by their asymptotic expansions for small argument. This is equivalent to writing each variable as a power series in $R$,

$$v_s = v_s^{(0)} + R\,v_s^{(1)} + R^2\,v_s^{(2)} + \ldots\ldots , \tag{3a}$$

$$v_R = v_R^{(0)} + R\,v_R^{(1)} + R^2\,v_R^{(2)} + \ldots\ldots , \tag{3b}$$

$$p = p^{(0)} + R\,p^{(1)} + R^2\,p^{(2)} + \ldots\ldots , \tag{3c}$$

where the coefficients are functions of s and t only. Equation (2a) implies that $v_R^{(0)}$ must be zero, which, together with equation (2b), implies that $p^{(1)}$ is zero, and this, together with equation (2c), implies that $v_s^{(1)}$ is zero.

The plane wave approximation which is valid for very long pulses is obtained by truncating the series (3) after the O (1) terms in the velocity and after the O (R) term in the pressure, so that the axial velocity and the pressure are uniform across each cross section of the tube and there is no radial velocity. An improved approximation, which is valid for moderately long pulses as well as very long pulses, is obtained by truncating the series (3) after the O (R) terms in the velocity and after the O ($R^2$) terms in the pressure so that the axial velocity is still uniform, but there is now a radial velocity which is proportional to R and a radial variation in the pressure which is proportional to $R^2$. Lin and Morgan [3] point out that when two terms are kept in their asymptotic expansions, the radial velocity is proportional to R. Once $p^{(2)}$ is known, $v_s^{(2)}$ can be obtained from equation (2c), so that O ($R^2$) terms could be kept for $v_s$ with very little extra effort, but it turns out that $v_s^{(2)}$ plays no significant role in the solution to this order of approximation.

The usual approximations for axisymmetric, small-deformation, elastic, plane-stress problems are assumed to hold for the thin-walled tube, so that the equations governing its motion are

$$\sigma_s = E^* (\epsilon_s + \nu \epsilon_\theta), \qquad \sigma_\theta = E^* (\epsilon_\theta + \nu \epsilon_s), \tag{4a, b}$$

$$\epsilon_s = \partial u/\partial s, \qquad \epsilon_\theta = w/r_m, \tag{4c, d}$$

$$\rho_t \, \partial \dot{u}/\partial t = \partial \sigma_s/\partial s, \tag{4e}$$

$$\rho_t \, r_m \, e \, \partial \dot{w}/\partial t = r \, p_w - \sigma_\theta \, e. \tag{4f}$$

In these equations, $\sigma_s$, $\sigma_\theta$, $\epsilon_s$, $\epsilon_\theta$, u and w are the axial stress, azimuthal or hoop stress, axial strain, azimuthal or hoop strain, axial displacement and radial displacement respectively, all of which are functions of s and t only. For the tube material,

$$E^* = E/(1 - \nu^2),$$

where E, $\nu$ and $\rho_t$ are the Young's modulus, Poisson's ratio and density respectively. For the undeformed tube, r is the inside radius, D is the outside diameter, e is the wall thickness and $r_m$ is the mean radius ( = D/2 - e/2). In addition, $p_w$ is the fluid pressure on the inside surface of the tube, and the dot denotes differentiation with respect to time, so that $\dot{u}$ and $\dot{w}$ are the axial and radial tube velocities respectively, which turn out to be the basic tube variables rather than u and w.

The fluid and tube problems are coupled by the pressure $p_w$ and by the inviscid boundary condition that the fluid velocity normal to a solid boundary equals the boundary's velocity in the same direction. In the context of the small-displacement and long-pulse approximations, this boundary condition and $p_w$ are

$$\dot{w} = v_R\,(R = r) = r\,v_R^{(1)},$$

$$p_w = p\,(R = r) = p^{(0)} + r^2\,p^{(2)}.$$

Thus $v_R^{(1)} = \dot{w}/r$ and this, together with the radial momentum equation (2b) for the fluid, gives

$$p^{(2)} = -(\rho_f/2)\,\partial v_R^{(1)}/\partial t = -(\rho_f/2r)\,\partial \dot{w}/\partial t.$$

Since $v_R^{(1)}$ and $p^{(2)}$ are determined by $\dot{w}$, they need not be kept as independent variables. Henceforth $p^{(0)}$ and $v_s^{(0)}$ will be denoted simply by p and v respectively, where both are functions of s and t only. Thus the series (3) become

$$v_s\,(R, s, t) = v + O\,(R^2), \tag{5a}$$

$$v_R\,(R, s, t) = (R/r)\,\dot{w} + O\,(R^2), \tag{5b}$$

$$p\,(R, s, t) = p - (\rho_f R^2/2r)\,\partial \dot{w}/\partial t + O\,(R^3), \tag{5c}$$

while the pressure driving the radial tube motion is

$$p_w = p - (\rho_f\, r/2)\,\partial \dot{w}/\partial t. \tag{5d}$$

It should be remembered that $p$ and $v$ in the subsequent analysis represent the pressure and axial velocity at the tube centerline $R = 0$, and that values elsewhere in the fluid differ by $O(R^2)$ terms.

The introduction of the expressions (5) into equations (2a, c, 4f) and of the expressions (4c, d) into equations (4a, b), together with the differentiation of equations (4a, b) with respect to time, gives six linear, first-order, hyperbolic, partial differential equations,

$$(1/K)\,\partial p/\partial t + (2/r)\,\dot{w} + \partial v/\partial s = 0\,, \tag{6a}$$

$$\partial\sigma_s/\partial t - E^*\,(\partial\dot{u}/\partial s + \nu\dot{w}/r_m) = 0\,, \tag{6b}$$

$$\partial\sigma_\theta/\partial t - E^*\,(\dot{w}/r_m + \nu\,\partial\dot{u}/\partial s) = 0\,, \tag{6c}$$

$$\rho_f\,\partial v/\partial t + \partial p/\partial s = 0\,, \tag{6d}$$

$$\rho_t\,\partial\dot{u}/\partial t - \partial\sigma_s/\partial s = 0\,, \tag{6e}$$

$$(\rho_t\,r_m\,e + \rho_f\,r^2/2)\,\partial\dot{w}/\partial t - r\,p + e\sigma_\theta = 0\,, \tag{6f}$$

governing the six independent variables, $p$, $v$, $\sigma_s$, $\sigma_\theta$, $\dot{u}$ and $\dot{w}$, which are functions of $s$ and $t$ only. Physically, a radial tube acceleration implies a radial fluid acceleration which increases linearly from zero at $R = 0$ to $\partial\dot{w}/\partial t$ at $R = r$, and the effect of this fluid acceleration appears as an added mass term in the first term of the radial momentum equation (6f) for the tube.

The equations (6) can be solved using the method of characteristics. There are two families of propagating characteristics and two other non-propagating characteristics, so that discontinuities must either remain stationary or propagate at either the speed of sound in the liquid $c_f$ or at the speed of sound in the tube material

$$c_t = (E^*/\rho_t)^{\frac{1}{2}}\,.$$

The modified wave speed used in the classical waterhammer approach (see e.g., [1]) is less than $c_f$ and is clearly not a true wave speed at which discontinuities or wave fronts can propagate.

The equations (6) are non-dimensionalized and transformed into the ordinary differential equations which hold along characteristics, giving

$$d\sigma_s \mp d\dot{u} - (\nu\dot{w}/r_m)\,dt = 0, \quad \text{along } ds/dt = \pm 1, \tag{7a}$$

$$(E^*/K)\,dp \pm (1/\gamma)\,dv + (2\dot{w}/r)\,dt = 0, \quad \text{along } ds/dt = \pm \gamma, \tag{7b}$$

$$\left.\begin{aligned} &\nu\,d\sigma_s - d\sigma_\theta + (1-\nu^2)(\dot{w}/r_m)\,dt = 0, &\text{(7c)}\\ &a\,d\dot{w} + (\sigma_\theta/r - p/e)\,dt = 0, &\text{(7d)}\end{aligned}\right\}\ \text{along } \frac{ds}{dt} = 0 .$$

In these equations, $s$, $r$, $r_m$ and $e$ have been normalized with respect to $D$; $t$ has been normalized with respect to $D/c_t$; $\dot{u}$, $\dot{w}$ and $v$ have been normalized with respect to $c_t$; and $p$, $\sigma_s$ and $\sigma_\theta$ have been normalized with respect to $E^*$. The non-dimensional wave speeds, which are equal to the slopes $ds/dt$ of the propagating characteristics, are equal to one and

$$\gamma = c_f/c_t = (K\,\rho_t/E^*\,\rho_f)^{\frac{1}{2}} .$$

In addition

$$a = (r_m/r) + (\rho_f\,r/2\rho_t\,e) .$$

## 3. Results for a water-filled copper tube

For a given tube, liquid and set of end conditions, the equations (7) can be solved numerically using finite differences. Here the tube is made of copper and has an outside diameter of 12.7 mm and a wall thickness of 0.76 mm (a standard 0.5 in. OD copper tube), the liquid is water and the end conditions are those for a semi-infinite tube with a prescribed force $f(t)$ on the capped end, which is taken to be at $s = 0$. (See Fig. 2). The cap is a massless, rigid plate with a frictionless seal between it and the end of the tube, so that equation (7d) is applied at $s = 0$. If the tube were rigidly attached to the cap, equation (7d) would not be applied at $s = 0$ and the end condition $\dot{w} = 0$ at $s = 0$ would be added to the conditions (9) given below. The applied force is

$$f(t) = \begin{cases} 0, & \text{for } t < 0 \text{ and } t \geq T, \\ f_o \sin(\pi t/T), & \text{for } 0 \leq t < T, \end{cases} \tag{8}$$

where $f$ has been normalized with respect to $E^* D^2$. Since the problem is linear, $f_o$ is set equal to one, so that the solution for any $f_o$ is given by $f_o$ times the present solution. Here $T$ is the non-dimensional pulse duration corresponding to a dimensional pulse duration of $T\,D/c_t$. If $\gamma \lesssim 1$, as it is for a water-filled copper tube, then the leading edge of the pulse generated by $f$ travels at a speed of $c_t$ and has propagated along the tube a distance equal to $TD$ by the time the applied force ends at $t = T$. Thus $T$ also characterizes the pulse length and, if $T = 20$, the pulse may be thought of as a 20-diameter pulse. The end conditions are

$$\left.\begin{aligned} \pi(r^2 p - 2r_m e\sigma_s) &= f, & \text{(9a)} \\ v &= \dot{u}, & \text{(9b)} \end{aligned}\right\} \text{ at } s = 0,$$

and the initial conditions are that all variables equal zero at $t = 0$.

The time variations of $p$, $\sigma_s$ and $\sigma_\theta$ at two gage locations, $s = 10$ and $s = 20$, are shown in Figs. 3 and 4 respectively for $T = 20$. Dimensional time in microseconds is used as the abscissa in order to provide a better physical picture of the pulse, while non-dimensional pressure and stress are used as the ordinates. These ordinates can be converted to dimensional values by multiplying by $f_o\,E^*$ where $E^* = 1.357 * 10^{11}\ N/m^2$. It should be noted that if $f_o$ was, in fact, equal to one, the peak applied force would be $2.19 * 10^8$ N, and the velocity and deformation would be so large that the acoustic and small-deformation approximations would not apply.

Figure 3 illustrates the fact that the main pressure pulse, which arrives at $s = 10$ at about $t = 80\ \mu$ sec, is preceded by a pressure dip associated with the faster moving compression pulse in the tube. Figure 4 shows that this precursor pressure dip has approximately the same shape at $s = 20$, while, as of $t = 160\ \mu$ sec, the main pressure pulse has not yet arrived.

Reducing the pulse duration $T$ from 20 to 2 has a drastic effect upon the pressure and stresses, whose time variation at two gage positions, $s = 5$ and $s = 10$, are shown in Figs. 5 and 6. It should be noted that the step sizes used for $t$ and $s$ in the finite difference approximation of equations (7) are proportional to $T$, so that the step sizes for $T = 2$ are one-tenth those for $T = 20$. For $T = 2$, there is no longer a well-defined precursor, and the hoop stress $\sigma_\theta$ no longer correlates well with the pressure as it did for $T = 20$. The question of whether the present analysis for a moderately long pulse applies for a 2-diameter pulse must be answered experimentally, and a program to do so is discussed in the conclusions.

## 4. Analytic solution for $c_f = c_t$

For at least one special case, the equations (6), together with the applied force (8) and the boundary conditions (9), can be solved analytically using Fourier sine and cosine transforms in $s$ and Laplace transforms in $t$. The equations (6) are normalized as described in section 2. Sine transforms are used for $v$ and $\dot{u}$, e. g.,

$$\bar{\bar{v}}\,(\xi,\ \eta) = \int_0^\infty \int_0^\infty \sin\,(\xi\ s)\ \exp\,(-\eta t)\ v\ (s,\ t)\ ds\ dt\ ,$$

while cosine transforms are used for $p$, $\dot{w}$, $\sigma_s$ and $\sigma_\theta$, e. g.,

$$\bar{\bar{p}}\,(\xi,\ \eta) = \int_0^\infty \int_0^\infty \cos\,(\xi\ s)\ \exp\,(-\eta t)\ p\ (s,\ t)\ ds\ dt\,.$$

The transforms of equations (6) are then

$$(E^*/K)\,\eta\,\bar{\bar{p}} + \xi\,\bar{\bar{v}} + 2\,\bar{\bar{\dot{w}}}/r = \bar{a}\ ,$$

$$\eta\,\bar{\bar{\sigma}}_s - \xi\,\bar{\bar{\dot{u}}} - \nu\,\bar{\bar{\dot{w}}}/r_m = -\,\bar{a}\ ,$$

$$\eta\,\bar{\bar{\sigma}}_\theta - \nu\,\xi\,\bar{\bar{\dot{u}}} - \bar{\bar{\dot{w}}}/r_m = -\,\nu\,\bar{a}\ ,$$

$$\rho_f\,\eta\,\bar{\bar{v}}/\rho_t - \xi\,\bar{\bar{p}} = 0\ , \qquad \eta\,\bar{\bar{\dot{u}}} + \xi\,\bar{\bar{\sigma}}_s = 0,$$

$$a\,\eta\,\bar{\bar{\dot{w}}} - \bar{\bar{p}}/e + \bar{\bar{\sigma}}_\theta/r = 0\ ,$$

where $\bar{a}(\eta)$ is the Laplace transform of the unknown function

$$a(t) = \dot{u}(0, t) = v(0, t) .$$

These six linear, algebraic equations are solved to obtain $\bar{\bar{v}}$, $\bar{\bar{u}}$, $\bar{\bar{w}}$, $\bar{\bar{p}}$, $\bar{\bar{\sigma}}_s$ and $\bar{\bar{\sigma}}_\theta$ in terms of $\bar{a}$.

Since $\bar{a}$ is independent of $\xi$, the Fourier inversion for all six variables can be carried out immediately, and, in particular, the Laplace transforms of the values of $p$ and $\sigma_s$ at $s = 0$ are given by the Fourier cosine inversions of $\bar{\bar{p}}$ and $\bar{\bar{\sigma}}_s$ for $s = 0$, e.g.,

$$\bar{p}(0, \eta) = (2/\pi) \int_0^\infty \bar{\bar{p}}(\xi, \eta)\, d\xi = \int_0^\infty \exp(-\eta t)\, p(0, t)\, dt .$$

The Laplace transform of the boundary condition (9a) gives

$$\pi \left(r^2 \bar{p}(0, \eta) - 2 r_m e \bar{\sigma}_s(0, \eta)\right) = \bar{f}(\eta) ,$$

where $\bar{f}$ is the Laplace transform of $f(t)$, namely

$$\bar{f} = \pi T (1 + \exp(-\eta T))/(\pi^2 + T^2 \eta^2) .$$

Introducing the expressions for $\bar{p}(0, \eta)$ and $\bar{\sigma}_s(0, \eta)$ in terms of $\bar{a}$ into the transform of the end condition (9a) determines $\bar{a}$, namely

$$\bar{a} = - i (P_1/Q_1 + P_2/Q_2)^{-1} \bar{f} , \tag{10}$$

where

$$P_1 = \eta (T_1 + T_2)/2F, \qquad P_2 = \eta (T_1 - T_2)/2F ,$$

$$T_1 = (A_t + A_f/W) F , \qquad T_2 = (A_t - A_f/W) Y - 4A_t ,$$

$$Q_1^2 = (F - B)/2Z , \qquad Q_2^2 = - (F + B)/2Z ,$$

$$F^2 = Y^2 + 8 e r_m W/r^2 ,$$

$$A_t = 2\pi r_m e, \qquad A_f = \pi r^2 ,$$

$$B = L(V + W)\eta^2 + M(XV + W) + N,$$

$$Y = L(V - W)\eta^2 + M(XV - W) + N,$$

$$Z = W(L + MX/\eta^2),$$

$$N = 2r_m/\nu r, \quad M = e/\nu r, \quad L = a e r_m/\nu,$$

$$V = E^*/K, \quad W = \rho_t/\rho_f, \quad X = 1 - \nu^2.$$

With $\bar{a}$ determined, the Laplace transforms of all six variables are known.

The solution (10) simplifies considerably for the special case of a tube material and fluid with equal speeds of sound, $c_t = c_f$ or $V = W$. For this case there are branch points at $\eta = \pm i r_1$ and at $\eta = \pm i r_2$ in the complex $\eta$-plane (See Fig. 7), where

$$r_1^2 = (1 + 2r_m/eV)/(a r r_m),$$

$$r_2^2 = X/(a r r_m) < r_1^2.$$

For $t > T$, the appropriate branch cuts are those shown in Fig. 7. For $0 < t < T$, the appropriate branch cuts would be from $+ir_1$ to $+i\infty$, from $-ir_2$ to $+ir_2$ and from $-i\infty$ to $-ir_1$. Only the solution for $a(t) = v(0, t) = \dot{u}(0, t)$ for $t > T$ is presented here, although solutions for the six variables for any $s$ and for any $t$, including $0 < t < T$, are given by equivalent Laplace inversion schemes. The Laplace inversion is given by an integral along the Bromwich path (See Fig. 7), which can be wrapped around the branch cuts. With the usual manipulations, this gives an integral expression for $a(t)$ $(= v(0, t))$, namely

$$a = C \int_{r_2}^{r_1} [\sin(xt) + \sin(x(t - T))]\, I(x)\, dx, \tag{11}$$

where

$$C = 2\,F\,T\,V\,N\,(1+U)^2/A_f\,,$$

$$I = (r_1^{\,2} - x^2)^{\frac{1}{2}}(x^2 - r_2^{\,2})^{\frac{1}{2}}(\pi^2 - T^2x^2)^{-1}\,(G\,(x) + H\,(x)\,)^{-1}\,,$$

$$G = U^2\,(1-N)^4\,(r_1^{\,2} - x^2)\,,$$

$$H = N^2\,(1+U)^4\,(x^2 - r_2^{\,2})\,,$$

$$U = e\,\nu\,E^*/r\,K = \nu^2\,M\,V\,,$$

and $F$ is now independent of $\eta$, namely

$$F = U + N\,.$$

The solution (11) can be used to check the numerical solution presented in section 3. First the numerical solution is obtained for $E^*/K = \rho_t/\rho_f = 50$, $e = 1$ mm, $D = 20$ mm, $\nu = 0.3$ and $T = 2$, and the values for $v\,(0,\,t)$ for $0 \leq t \leq 50$ are plotted as the dashed line in Fig. 8. Next the integral in the analytic solution (11) is evaluated numerically using a 48-point Gauss quadrature for discrete values of $t$ in the range $2 \leq t \leq 50$, and the values of $a\,(t)$ are plotted as the solid line in Fig. 8. The agreement is very good, the only discrepancy being a slight cumulative time delay in the solution using the method of characteristics. This delay is felt to be attributable to the finite size of the time increment used in the numerical solution [4].

## 5. Conclusions

The present problem has been chosen in order to emphasize the stress waves in the tube, particularly the main compression wave in the tube, which, for a 20-diameter pulse, travels faster than the main pressure pulse in the fluid and produces a negative-pressure precursor in the fluid. In the classical waterhammer problem, fluid is flowing through the tube initially and a valve at the downstream end of the tube is suddenly closed. If the valve is not rigidly attached to some fixed structure, the principal wave in the tube would be an axial expansion wave, which would produce a positive-pressure precursor ahead of the main pressure surge in the fluid. The stresses in the tube and the pressure in the precursor would, however, be much smaller, relative to the pressure in the main pressure surge, than in the present problem. Such small, positive-pressure precursors have been observed experimentally [5]. If the valve were rigidly fixed, there would be no expansion wave in the tube generated by a sudden closure. The main pressure surge would produce positive radial displacements, which would in turn spawn axial compression waves in the tube. These compression waves would travel faster than the main pressure surge and would produce negative-pressure precursors ahead of this surge in the fluid, but the pressure dip in these precursors may be quite small and therefore possibly difficult to detect experimentally.

The object of the present analysis is to develop an approximation for acoustic waves in elastic tubes which represents an improvement over the classical waterhammer approximation and which leads to equations that can be solved in a straightforward fashion using the method of characteristics. The first improvement is that the present analysis is not restricted to problems for which the speed of sound in the tube material $c_t$ is much larger than that in the fluid $c_f$, and in fact there are no restrictions on $c_f$ and $c_t$ here.

The second improvement is that classical waterhammer theory is restricted to very long pulses while the present theory also applies to moderately long pulses. At present the minimum pulse lengths for which the classical waterhammer theory and the present theory apply are not known, so the degree of improvement provided by the present theory is also unknown. An experimental apparatus capable of applying an impulsive force $f(t)$ to the end of a capped, water-filled, 0.5 in. O.D. copper tube is currently being constructed. The duration $T$ of the pulse will be controllable, while the values of $f(t)$ will be measured and fed into a computer program to predict the disturbance in both the tube and the fluid, using both classical waterhammer theory and the present theory. A comparison of numerical and experimental results will hopefully indicate the limits of both theories and the improvement provided by the present theory.

## Acknowledgments

This research was supported partly by Argonne National Laboratory under Contract U.S. University of Chicago / SC AEC 31-109-38-3056 and partly by the National Science Foundation under Grant ENG 74-23778.

## References

1. Streeter, V. L., and Wylie, E. B., Hydraulic Transients (McGraw-Hill Book Company, New York, 1967).
2. Walker, J. S., "Perturbation solutions for steady one-dimensional waterhammer waves," Journal of Fluids Engineering, 97 (2) (1975), pp. 260-262.
3. Lin, T. C., and Morgan, G. W., "Wave propagation through fluid contained in a cylindrical, elastic shell," Journal of the Acoustical Society of America, 28 (6) (1956), pp. 1165-1173.
4. Phillips, J. W., "Pulse propagation in a helix -- theory and experiment," Journal of Applied Mechanics, 41 (4) (1974), pp. 1047-1051.
5. Thorley, A. R. D., Pressure Transients in Hydraulic Pipelines, Journal of Basic Engineering, 91 (1969), pp. 453-461.

Figures



JSW:vs

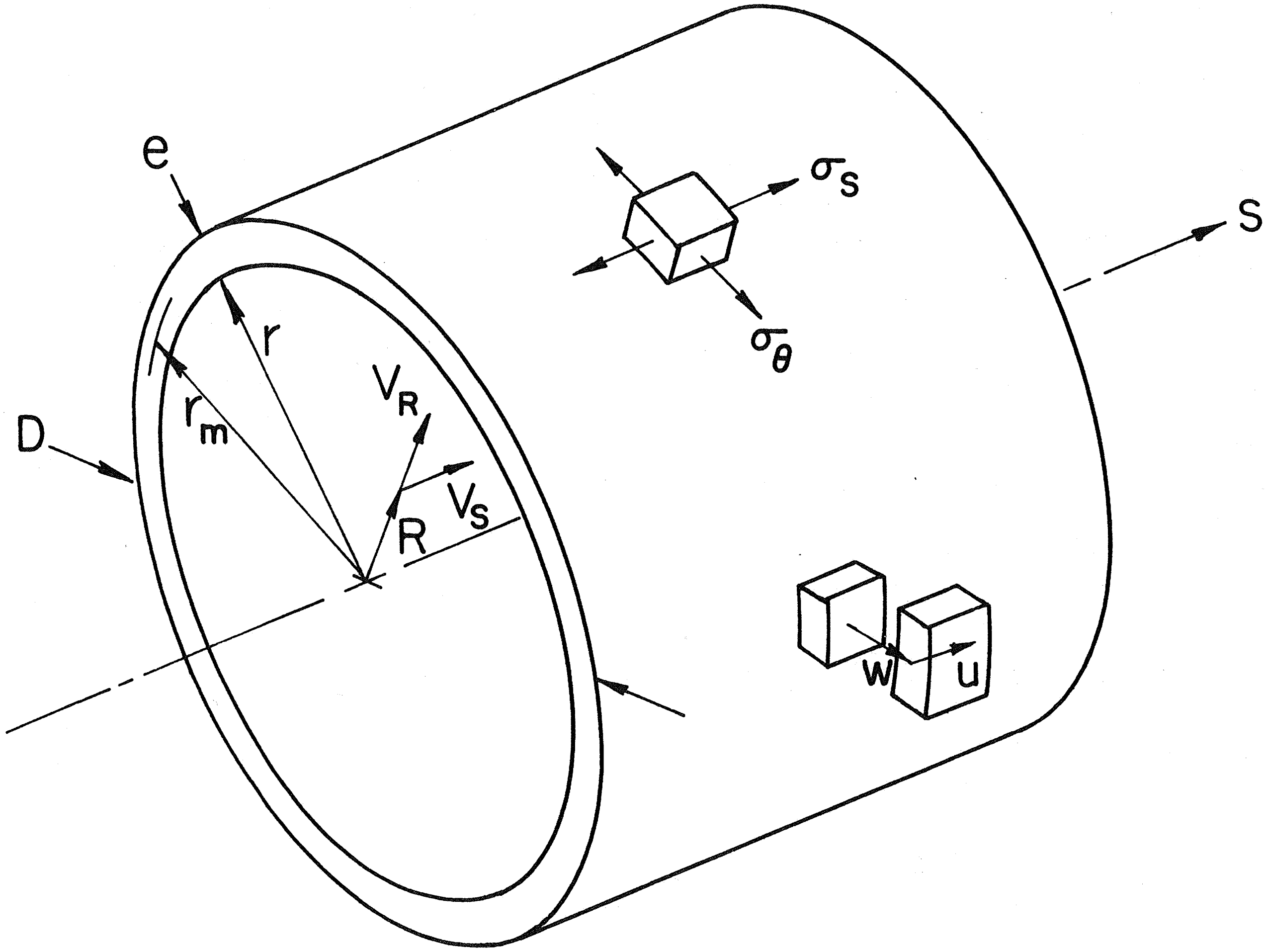


Fig. 1. Walker & Phillips

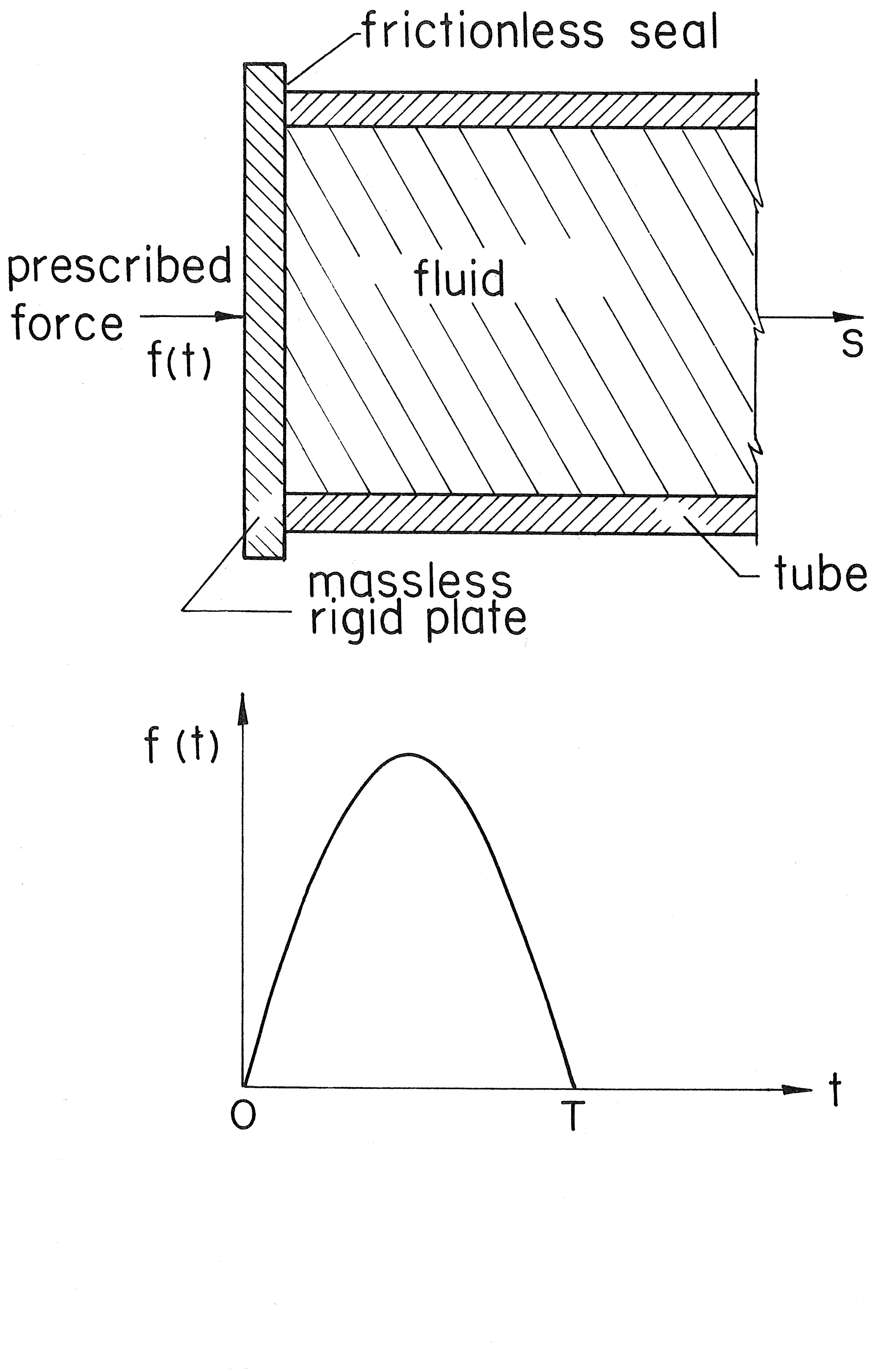


Fig. 2. Walker & Phillips

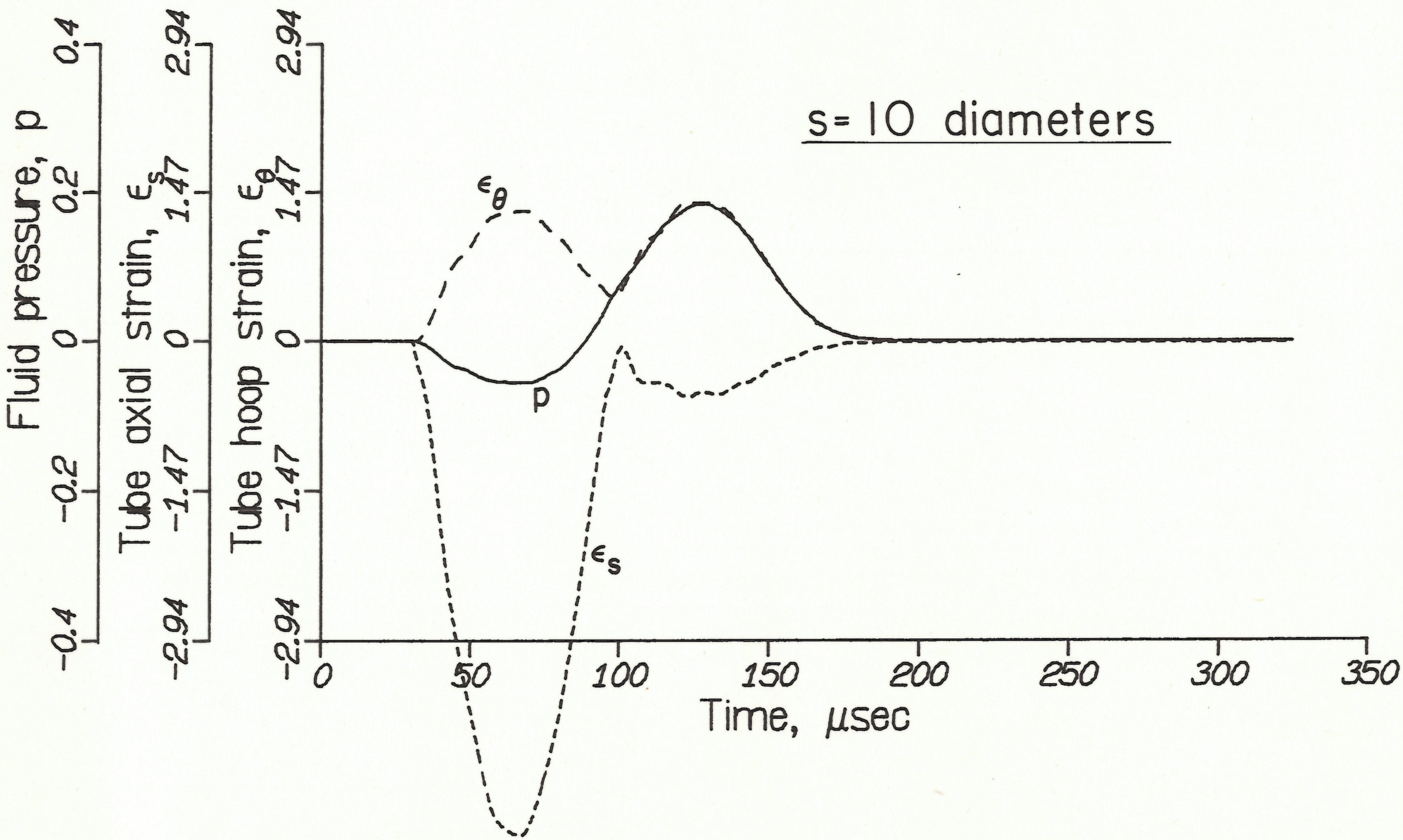


Fig. 3. Walker & Phillips

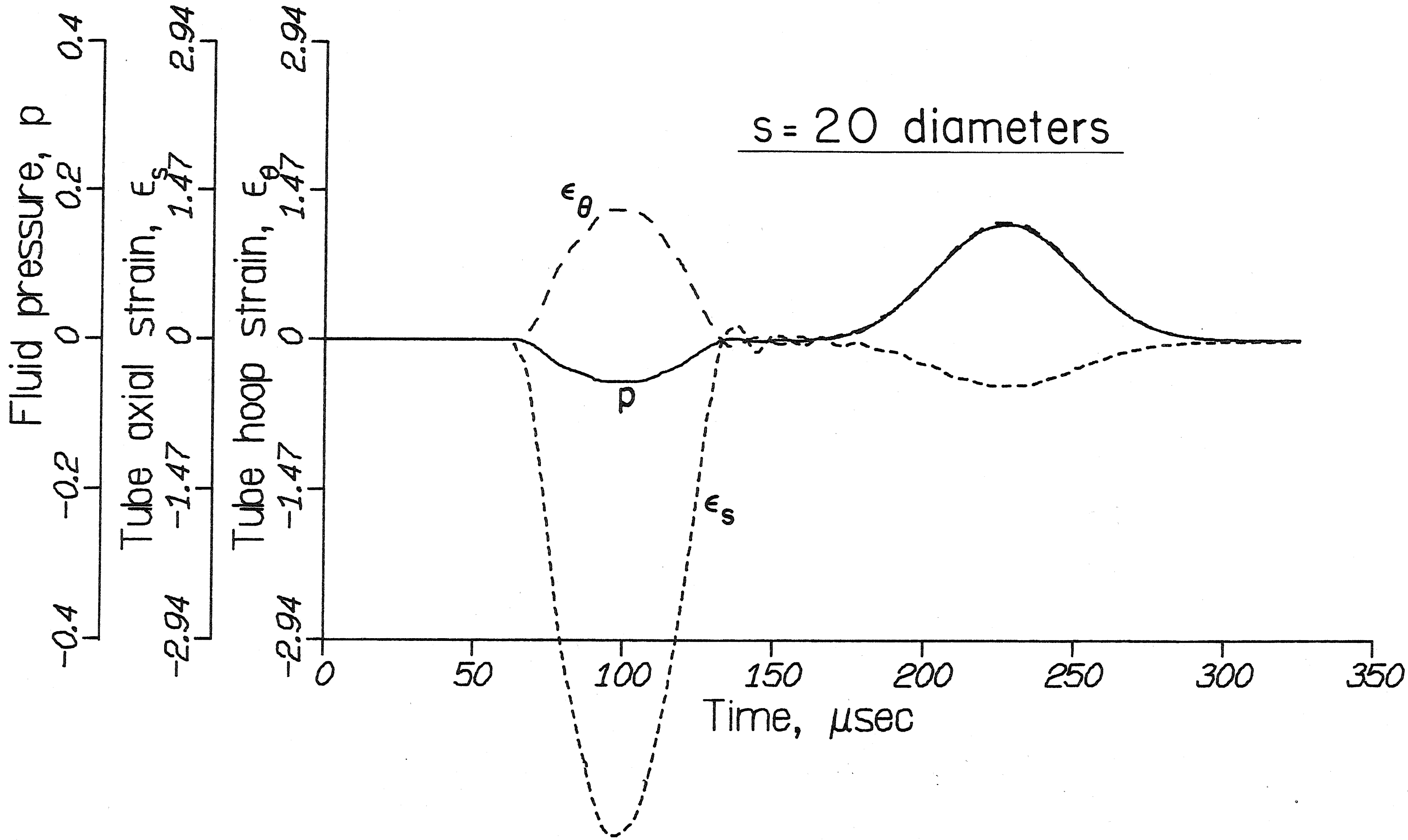


Fig. 4. Walker & Phillips

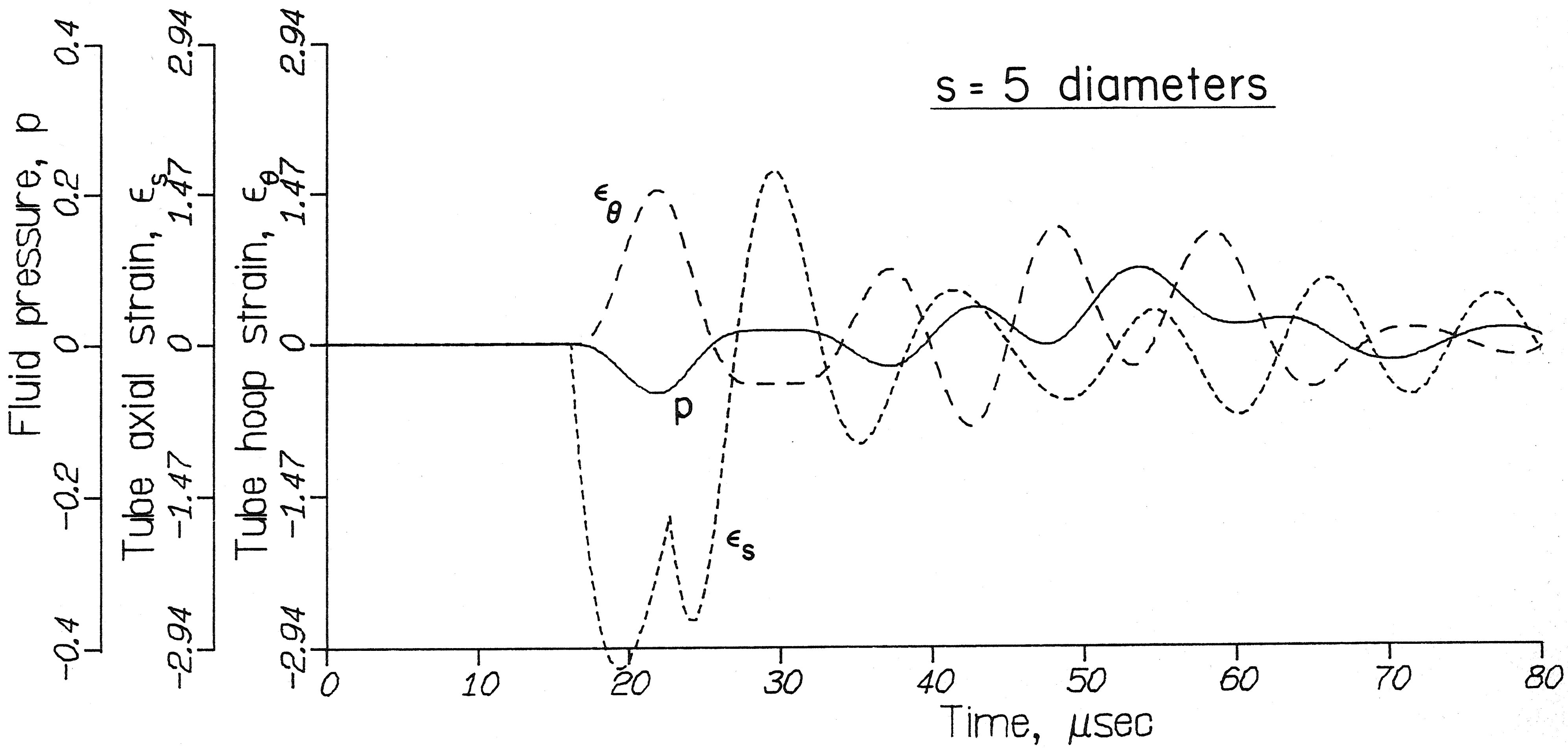


Fig. 5. Walker & Phillips

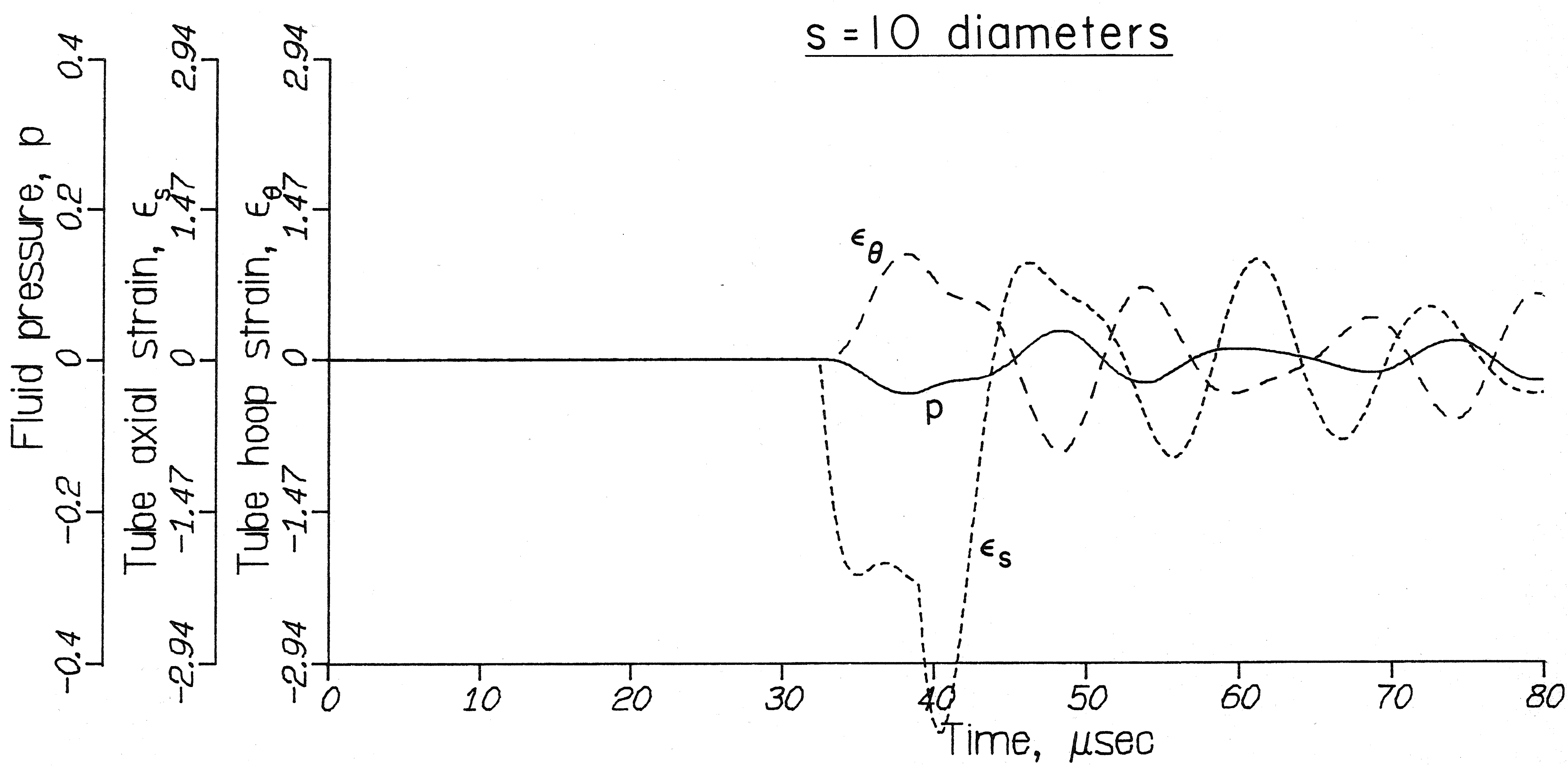


Fig. 6. Walker & Phillips

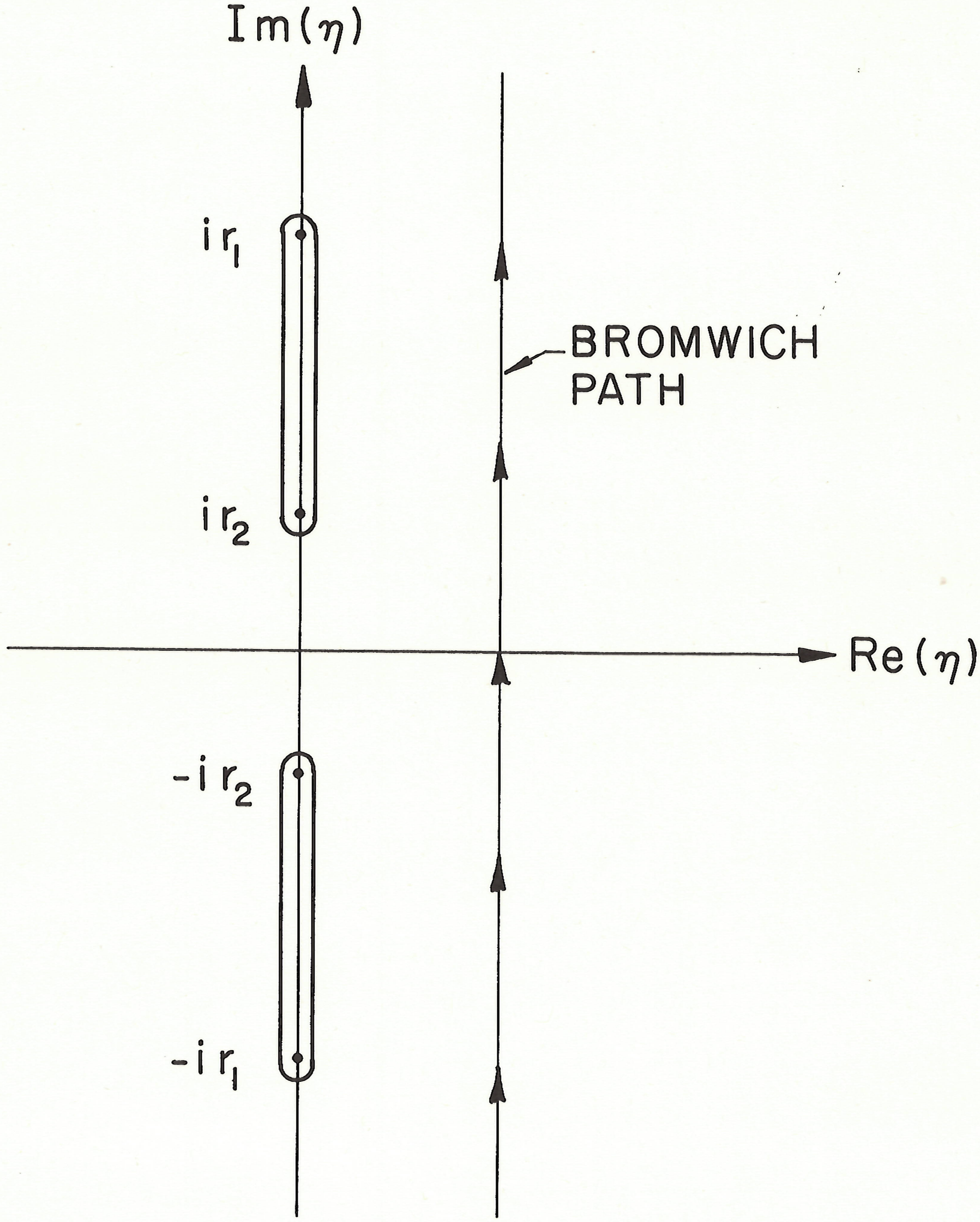


Fig. 7. Walker & Phillips

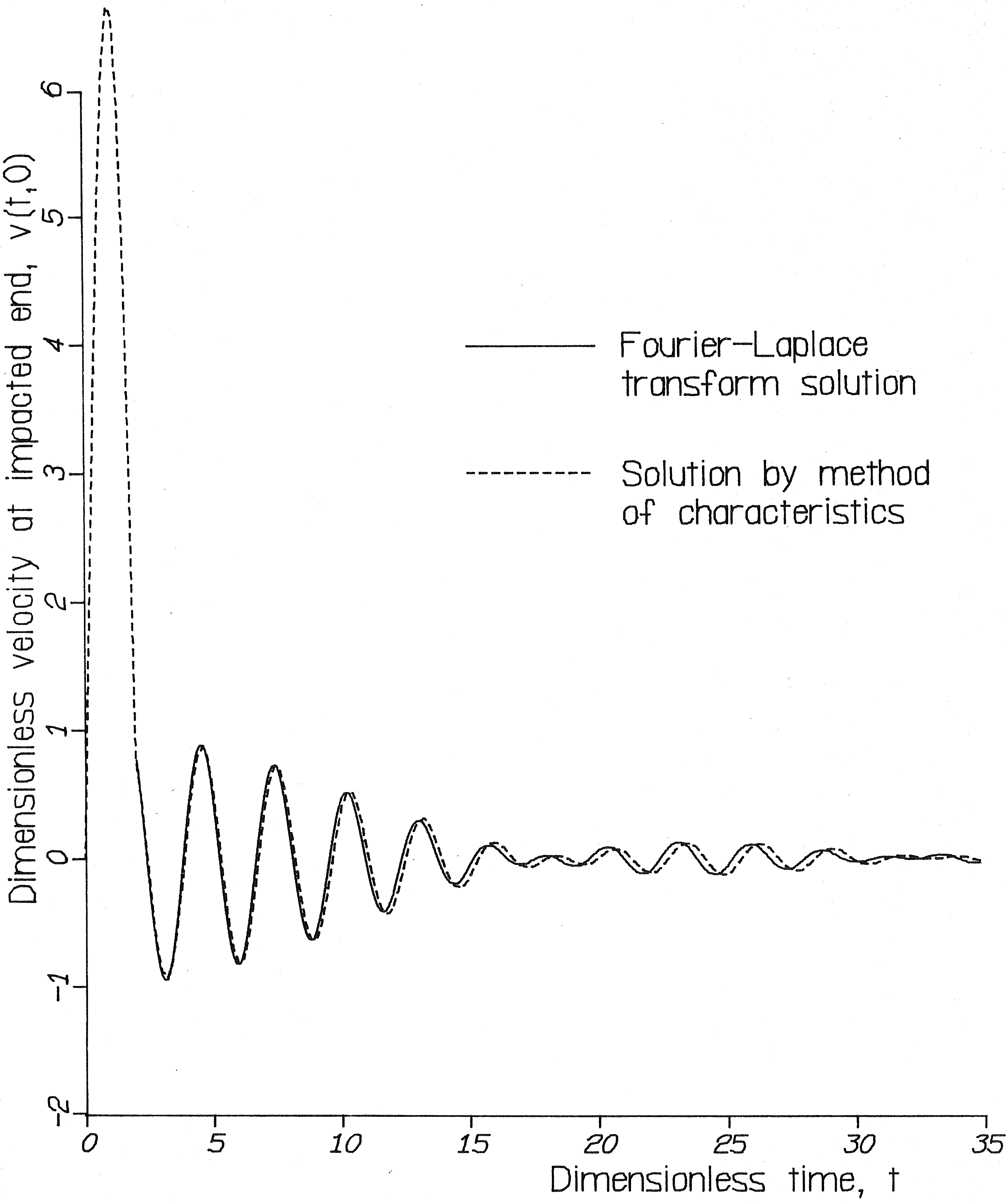


Fig. 8. Walker & Phillips